

SCATTERING OF ELECTRONS BY PROTONS

K. Berkelman, J. M. Cassels, D. N. Olson and R. R. Wilson

Laboratory of Nuclear Studies, Cornell University, Ithaca, New York

(presented by R. R. Wilson)

1. INTRODUCTION

The scattering of electrons by protons has been studied using the Cornell 1.3 BeV synchrotron. It is possible to make measurements in spite of the relatively weak intensity of the synchrotron by placing the scattering target directly into the circulating beam, in which case the electrons make many traversals on successive turns. Results are reported for values of q^2 , the square of the 4-momentum transfer, up to 25 f^{-2} , obtained at electron scattering angles of 66° and 112° . The data are in agreement with the Stanford 650 MeV results¹⁾ where they overlap. However, at higher values of q^2 the data suggest that F^2 , the ratio of the experimentally determined cross section to the point Mott cross section, varies with the scattering angle, and therefore that F_1 and F_2 , the electric and magnetic form factors of Rosenbluth, are not equal.

2. APPARATUS AND PROCEDURE

Figs. 1 and 2 show vertical and horizontal views of the general layout and of the counter telescope. The electron beam of the Cornell synchrotron spiraled inwards at the peak of the magnetic cycle as a result of controlled decrease of the radiofrequency accelerating voltage. For periods of about 1 ms, repeated 30 times per second, the electrons bombarded polyethylene or carbon targets in a scattering chamber located in one of the straight sections. The targets were in the form of rods about $1/16''$ square, disposed horizontally in the median plane of the synchrotron at an angle of 45° to the beam direction. The tips of the targets were 1.1 cm inside the normal equilibrium orbit of the beam. Discoloration of the poly-

ethylene showed that the targets were bombarded at distances up to $1/16''$ back from the tips.

A totally absorbing ion chamber, or quantameter²⁾, integrated absolutely the bremsstrahlung emitted from the target. Knowledge of the radiation length of the target materials at the various electron energies gives directly the effective product of the target thickness and the incident electron flux, which is the quantity required for cross section calculations. It was evident that on the average the electrons traversed the target about ten times before being finally lost from the synchrotron.

Photographs were taken of the bremsstrahlung spot immediately in front of the ion chamber. Usually these showed a clean spot about $1/4''$ in diameter, which checked that electrons were not hitting objects, other than the targets, in or near the scattering chamber. In the early stages of the experiment a second diffuse spot was sometimes caused by electrons hitting a beam-detecting device at the upstream entrance to the chamber; this improper mode of operation was associated with incorrect monitoring and low measured cross sections. The trouble was eliminated by adjustment of the in-phase correction coils which steer the synchrotron beam at high energies.

Scattered electrons, or recoil protons, left the scattering chamber through a $0.005''$ Mylar window and were then deflected magnetically by a single quadrupole lens. This produced vertical focusing of the particles passing over or under a central obstacle $3.7''$ high, made of lead and copper. The momentum window of the spectrometer was defined by this obstacle and by the plastic scintillator defining counter, whose maximum height was $1/8''$. In vertical section

this scintillator had the shape of a truncated diamond, in order to obtain the best possible bias curve for the pulses. The quadrupole lens was of course defocusing horizontally, and therefore this scintillator was made 8" wide.

In a typical run the collected particles were emitted at semihorizontal angles up to 0.97° , measured at the target with respect to the central ray; the total solid angle collected by the spectrometer was 4.41 millisteradians. The momenta of the particles varied with the horizontal angle of emission, an effect which was only appreciable for recoil protons. To compensate for it, the defining counter was turned through a small angle (e.g., 18° at 1205 MeV) round its vertical axis, counterclockwise as seen from above.

For a point target on the axis the theoretical curve of detection efficiency versus magnetic field gradient,

for a fixed momentum particle, was trapezoidal in shape. It had an almost flat top and a typical full width of 3.1% at half efficiency. In practice the resolution curve was smeared by the finite height of the target and various multiple scattering processes, especially for recoil protons. However, the area under the peak should not be seriously changed by these effects, and so the cross sections were computed by integrating peaks in the experimental counting rate as a function of magnetic field gradient. Actually the voltage across a shunt in series with the exciting coils of the magnet was used as the independent variable, and the areas multiplied by an appropriate constant. At the highest momenta the field gradients were not quite proportional to the exciting currents, and a differential correction ($\lesssim 9\%$) was made for this.

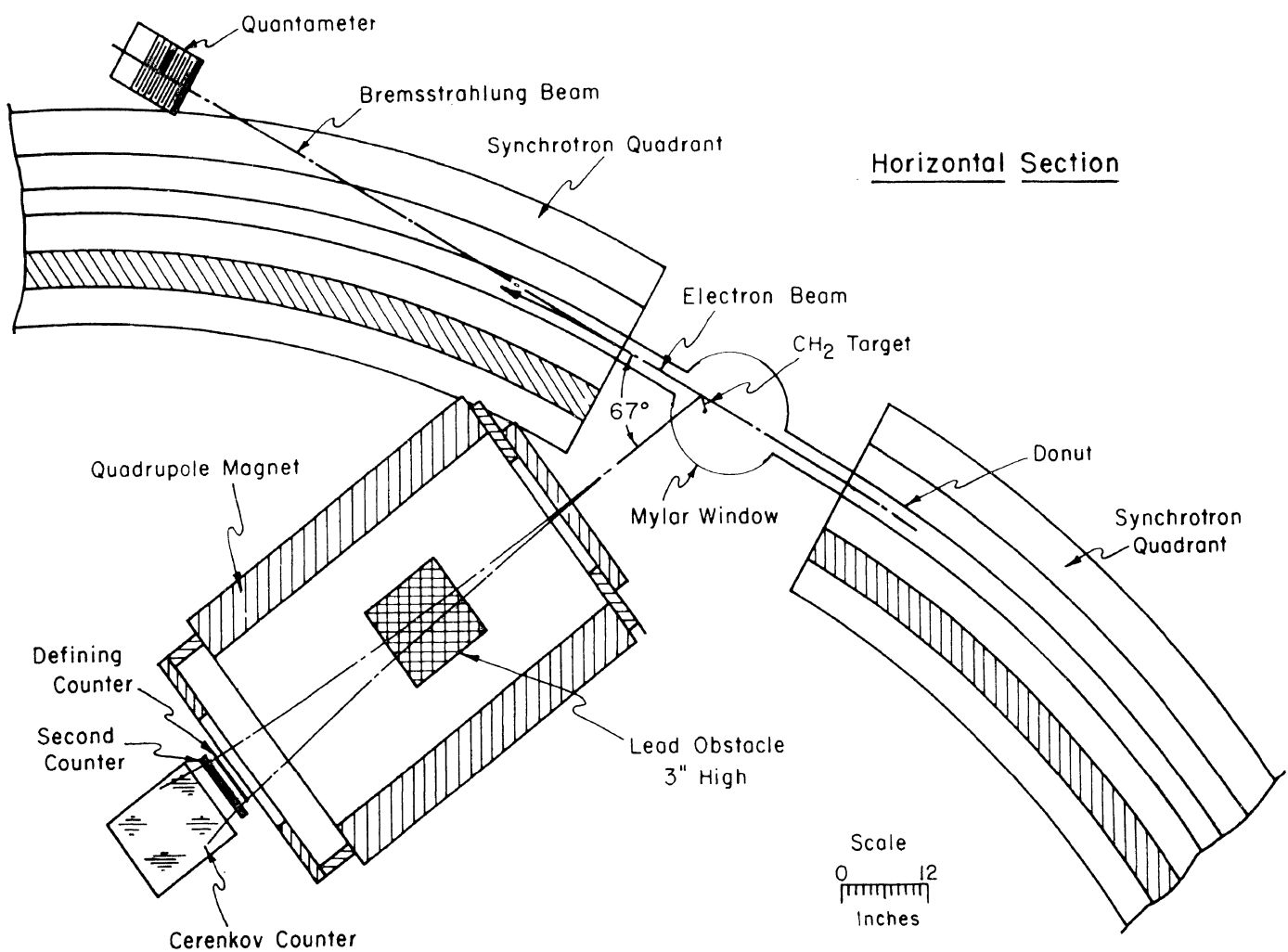


Fig. 1 Plan view of the apparatus described in the text.

The procedure just outlined was used for (a) the 66° scattering of 587, 684, 781, 879, and 1034 MeV electrons, (b) the 112° scattering of 320 and 261 MeV electrons, and (c) the protons recoiling at 66° from the scattering of electrons with energies of 684, 781, 982, 1034, 1173, and 1205 MeV.

The counting rate was measured only in the region of the peak for (d) the 66° scattering of 982, 1085, 1173, and 1215 MeV electrons, and (e) the 112° scattering of 909 MeV electrons. The corresponding cross sections were evaluated using the line shape established in the full sets of measurements.

The other two counters in the telescope were used to reduce backgrounds. The Čerenkov counter was inoperative when the comparatively slow recoil protons were being detected, and the bias on the second plastic scintillator was raised so that relativistic particles were not detected. Coincidences between the two scintillation counters were required, the effective pulse widths being about $0.5 \mu\text{s}$.

When electrons were being detected, the bias on the second scintillator was lowered, and the Čerenkov

counter was brought into operation. This was a lead glass total absorption detector, which produced recognizably large pulses when the desired electrons arrived. Triple coincidences between the three counters were required, the effective width of the mixed pulses being about 20 ns for the defining counter, 200 ns for the Čerenkov counter, and $0.7 \mu\text{s}$ for the middle counter. Each triple coincidence event opened an electronic gate, allowing the output from the Čerenkov counter to reach a pulse height analyzer.

3. RESULTS

Figs. 3 and 4 show respectively the recoil proton and the scattered electron peaks observed at 66° from 781 MeV incident electrons. The ordinates are the coincidence counts observed per "sweep" of the quantameter (1 sweep = 4.97×10^{12} MeV), and the abscissae are the voltages in the spectrometer shunt. The carbon target results have been multiplied by a normalizing factor $\beta = 0.89$, which equalizes the

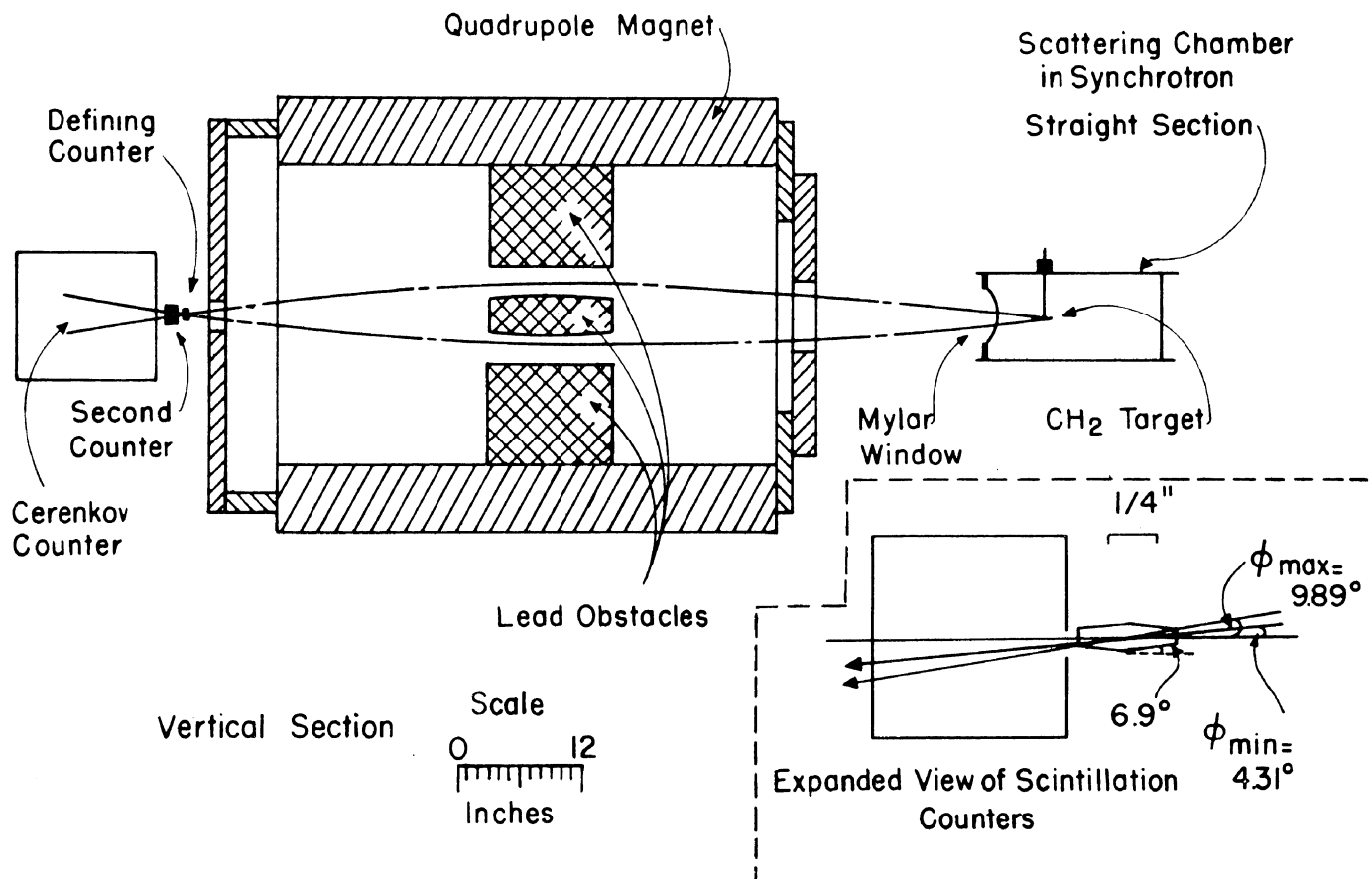


Fig. 2 Side view of the target, spectrometer, and counter telescope. The inset shows an enlarged view of the two scintillation counters.

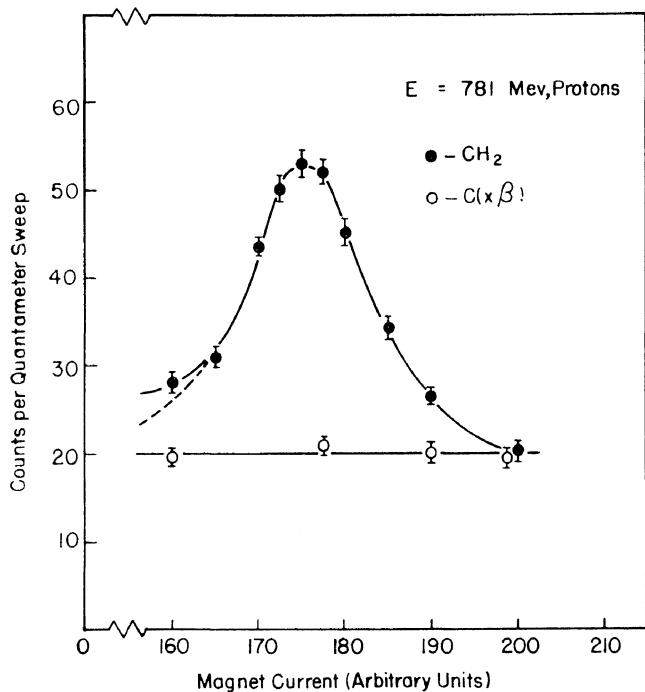


Fig. 3 The counting rate as a function of magnet current; protons recoiling at 66° from collisions of 781 MeV incident electrons.

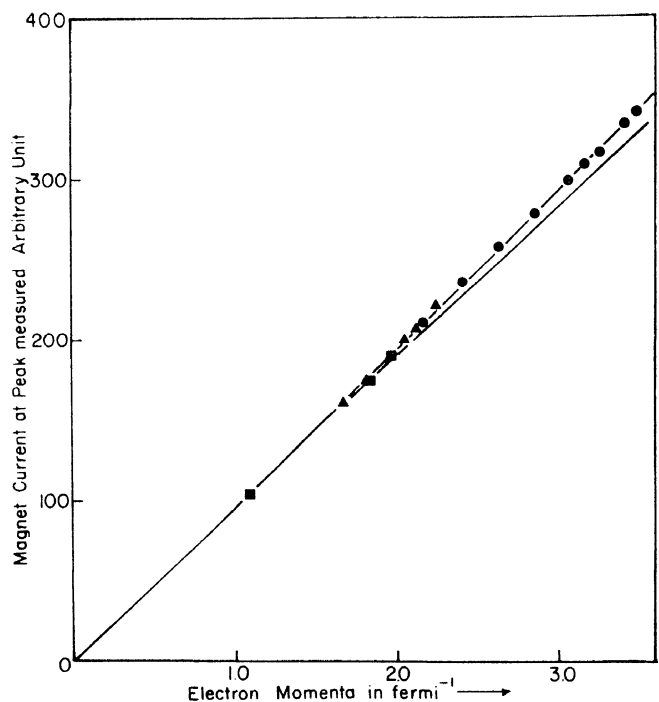


Fig. 5 Magnet current at the top of the peak, plotted against expected momenta of the particles. The difference between the straight line and the line through the points represents saturation effects.

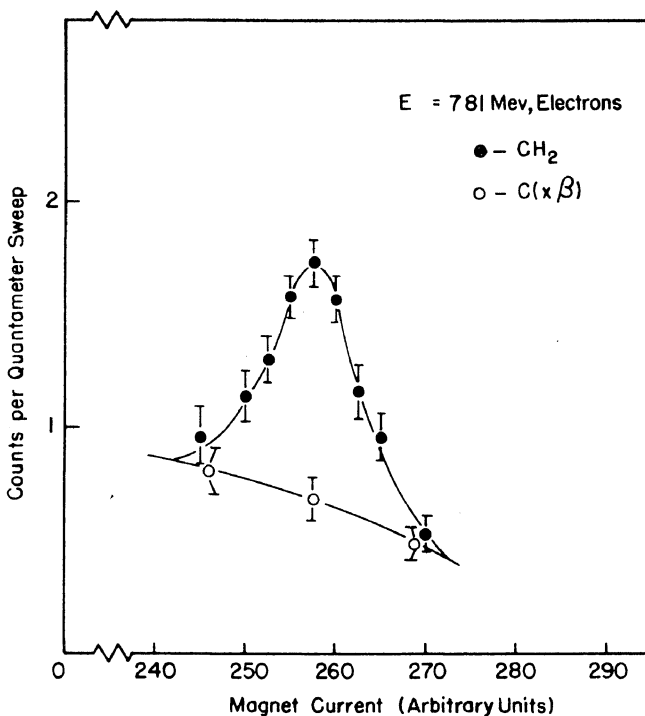


Fig. 4 The counting rate as a function of magnet current; electrons scattered at 66° from collisions of 781 MeV incident electrons.

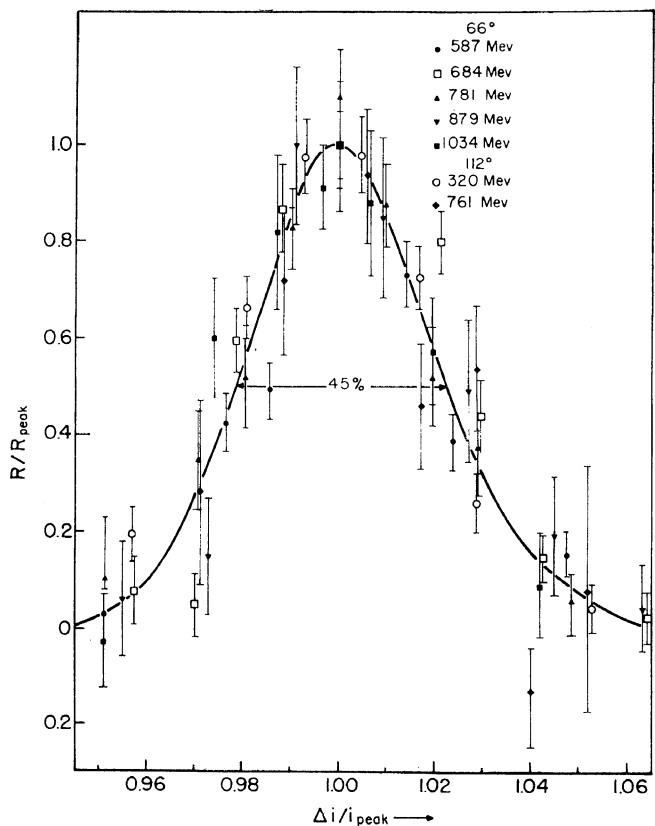


Fig. 6 Line shape of the peaks caused by elastically scattered electrons.

effects of the carbon nuclei in the two target materials. Rather clean elastic peaks are revealed in both figures, although there is a small inelastic tail in the proton distribution.

Fig. 5 shows a plot of the positions of the peaks versus the theoretical momenta of the particles being detected, the assumption being of course that these come from elastic electron-proton scattering. The points lie on an almost straight line whose slope checks correctly with independent fluxmeter measurements of the spectrometer magnetic field. Fig. 6 shows the line observed in all the complete sets of electron measurements, before correction for saturation.

It was found that the height of a peak decreased slowly if a given polyethylene target was bombarded for a long time. Presumably this was due to ejection of the hydrogen from the target, an effect probably correlated with a brownish discoloration which also appeared. The polyethylene targets were changed

every few hours and a suitable correction for aging was established and applied ($\lesssim 3\%$).

Finally the usual radiation correction ($\lesssim 13\%$) was applied to allow for the emission of bremsstrahlung in the electron-proton scattering process.

The results, expressed as a plot of F^2 against q^2 , are shown in Fig. 7. For comparison the highest results of Hofstadter et al¹⁾ taken with the Stanford linac, operated at 550, 600, and 650 MeV, are shown, as well as the recent values determined by L. N. Hand³⁾ at 135° and 850 MeV.

4. DISCUSSION

The results of the present experiment clearly agree well with the Stanford data wherever they overlap, that is for $q^2 \lesssim 11 \text{ f}^{-2}$ when $\theta < 90^\circ$, and for $q^2 \lesssim 17 \text{ f}^{-2}$ when $\theta > 90^\circ$. Often the form factors at low q^2 are expanded in the static approximation,

$$F_{1,2} = 1 - \frac{1}{6} \langle a_{1,2}^2 \rangle q^2 + \dots \quad (4)$$

where $a_{1,2}$ are the r.m.s. radii of the charge and the anomalous magnetic moment of the proton. Thus no change is indicated in the conclusion of Hofstadter et al that these radii are about 0.8 f. It should be noted, however, that Eq. (4) is subject to relativistic and dynamic corrections of the order of q^2/M^2 , so that the exact physical significance of this line of interpretation is not very clear.

At high values of q^2 the points for $\theta < 90^\circ$ (circles in Fig. 7) seem to be consistently higher than the points for $\theta > 90^\circ$ (crosses in Fig. 7). This trend indicates that F_1 and F_2 are not equal; in fact, the results at $q^2 = M^2 = 22 \text{ f}^{-2}$ would be well fitted with $F_2 \sim \frac{1}{4} F_1$. Indeed at $q^2 = 19$, $F_2/F_1 = 0.1 \pm 0.2$ and at $q^2 = 25$, $F_2/F_1 = 0 \pm 0.3$. However, the corresponding results for electron-neutron scattering are needed before much further progress can be made in relating experimental results to the dispersion theory^{4, 5)} of electron-nucleon scattering.

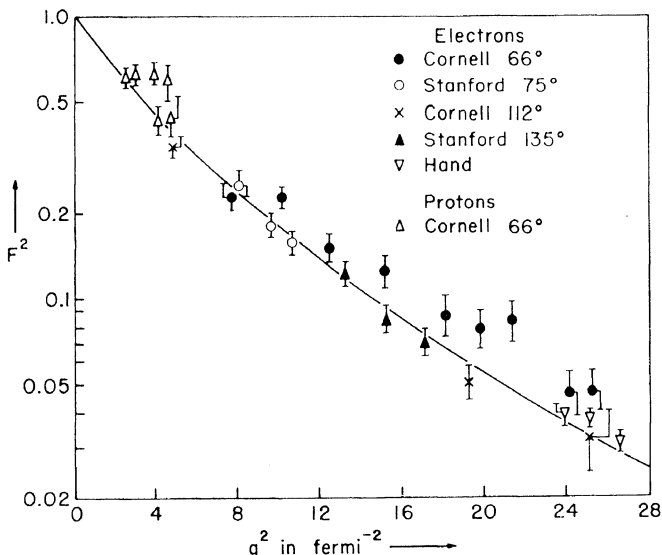


Fig. 7 Experimental results, including data from the work of Hofstadter et al. The proton points correspond to forward scattering of the electrons, with low q^2 . The solid line, drawn only for convenient reference, is given by the formula $F^2 = [1 - 0.0533q^2]^{-4}$.

LIST OF REFERENCES AND NOTES

1. Hofstadter, R., Bumiller, F. and Yearian, N. R. Rev. Mod. Phys. **30**, p. 482 (1958).
2. Wilson, R. R. Nuclear Instr. **1**, p. 101 (1957).
3. Hand, L. N. Phys. Rev. Letters **5**, 168 (1960).
4. Chew, G. F., Karplus, R., Gasiorowicz, S. and Zachariasen, F. Phys. Rev. **110**, p. 265 (1958).
5. Federbush, P., Goldberger, M. L. and Treiman, S. B. Phys. Rev. **112**, p. 642 (1958).